

# Solid-state NMR and wide-angle X-ray diffraction study of hydrofluoroether/ $\beta$ -cyclodextrin inclusion complex

Yusuke Koito · Kazuhiko Yamada ·  
Shinji Ando

Received: 25 November 2011 / Accepted: 18 May 2012 / Published online: 20 June 2012  
© Springer Science+Business Media B.V. 2012

**Abstract** An inclusion complex (IC) composed of a hydrofluoroether (HFE) guest and a  $\beta$ -cyclodextrin ( $\beta$ -CD) host was newly prepared, and the crystalline structure and the thermal stability of the IC were examined using several analytical methods, including wide-angle X-ray diffraction (WAXD), solid-state NMR, thermogravimetric analysis (TGA), TG–mass spectrometry (TG–MS), and quantum chemical calculation. The WAXD patterns and elemental analysis identified that the IC of an HFE/ $\beta$ -CD form of a channel-type structure, in which one HFE molecule is included in a common cavity of two  $\beta$ -CD molecules. TGA and TG–MS analysis indicated that the HFE molecules included in  $\beta$ -CD are hardly evaporated or degraded up to the decomposition temperature of the  $\beta$ -CD host. Solid-state  $^{13}\text{C}$  NMR indicated that the  $\beta$ -CD ring structure was deformed by including an HFE molecule in it, and that the  $^{19}\text{F}$  NMR signals of the HFE guest were significantly shifted to higher frequencies by the inclusion due to the dielectric media effect in the cavity of  $\beta$ -CD. Moreover, the  $^{19}\text{F}$  NMR signals of HFE included in IC were further shifted after annealing at 150 °C, which reflected structural changes in HFE/ $\beta$ -CD IC caused at elevated temperatures. The WAXD patterns also confirmed that the packing structure along the crystalline *b*-direction of HFE/ $\beta$ -CDs, which penetrates the cavities of  $\beta$ -CDs, was compressed by annealing and transformed to a more stable structure.

**Keywords** Solid-state NMR · Inclusion complex ·  $\beta$ -Cyclodextrin · Hydrofluoroether

## Introduction

Cyclodextrins (CDs) are cyclic oligosaccharides composed of six, seven, or eight D-glucose units linked by  $\alpha$ -(1→4) glycosidic bonds, forming a doughnut-shaped structure [1]. Because the inner wall of the structure is highly hydrophobic, a single CD or two CDs can capture various compounds into the cavity, which is known as a host–guest inclusion complex (IC) [2]. On the other hand, it has been reported [3] that several kinds of fluorine-containing compounds are harmful to natural environments. For example, chlorofluorocarbon is considered to destroy the ozone layer of the earth, is registered as a green-house gas and is no longer in production, although it had been widely used as a refrigerant, a solvent, and a detergent. As an alternative compound, hydrofluoroether (HFE), the risk of which to the environment is considerably lower than that of chlorofluorocarbons, has received considerable attention, and is currently used in a variety of industrial fields, including the manufacture of semi-conductor materials as dust and moisture removers, a fire-extinguishing agent and a dispersal medium for fluorine-containing compounds [4, 5]. However, it is desirable to remove them after use because decomposed components of HFE are generally harmful to the environment and the human body. CDs, crown-ethers [6] and calixarenes [7, 8], are expected to function as hosts of ICs, which capture and remove such harmful or toxic components dispersed in solutions. In particular, CD is an attractive and promising candidate for industrial purposes because of its low cost, ease of use, and good captive ability. The objective of this study is to investigate the structure and thermal stability of ICs consisting of  $\beta$ -CD as the host and HFE as the guest.

Solid-state nuclear magnetic resonance (NMR) is one of the most versatile tools for investigating the molecular

Y. Koito · K. Yamada · S. Ando (✉)  
Department of Chemistry and Materials Science, Tokyo Institute of Technology, Ookayama, Meguro-ku, Tokyo 152-8552, Japan  
e-mail: sando@polymer.titech.ac.jp

structures and dynamics of ICs. Tonelli and co-workers [9, 10] utilized  $^1\text{H} \rightarrow ^{13}\text{C}$  cross-polarization (CP)/magic-angle spinning (MAS) NMR to prove the formation of ICs and to characterize the molecular properties by analyzing  $^{13}\text{C}$  lineshapes and relaxation parameters, such as  $T_1^{\text{C}}$  and  $T_{1\rho}^{\text{C}}$ . Further, Saalwächter [11] reported that geometrical correlation was observed between a  $\gamma$ -CD host and a poly(-dimethyl siloxane) guest by using ultra high-speed MAS and multiple pulse  $^1\text{H}$  NMR. On the other hand, we have recently reported that a perfluoroalkane ( $\text{C}_9\text{F}_{20}$ )/ $\beta$ -CD IC can be easily obtained from a mixture of neat  $\text{C}_9\text{F}_{20}$  and a saturated aqueous solution of  $\beta$ -CD, and  $^1\text{H} \rightarrow ^{19}\text{F}$  CP/MAS NMR revealed that  $\text{C}_9\text{F}_{20}$  molecules included in  $\beta$ -CD undergo vigorous molecular motion above 80 °C and partly comes out of a  $\beta$ -CD channel [12]. However, the guests hardly degrade or evaporate unless the host is pyrolytically decomposed above ca. 300 °C. This very high thermal stability of the ICs is an important factor for industrial applications, and the structural changes in ICs occurring at elevated temperatures are worthy of investigation.

In this study, we report the preparation of a  $\beta$ -CD IC, including a HFE molecule for the first time, and clarify the structural properties using the  $^{19}\text{F}$  MAS and  $^1\text{H}(^{19}\text{F}) \rightarrow ^{13}\text{C}$  CP MAS NMR, and wide-angle X-ray diffraction (WAXD) techniques. Moreover, the thermal stability and structural changes of the IC are discussed based on solid-state NMR, WAXD, thermo gravimetric analyses (TGA) and thermo-gravimetry–mass spectroscopy (TG–MS).

## Experimental

### Materials

The chemical structure of the HFE compound used in this study is  $\text{CF}_3\text{--CFH--CF}_2\text{--CH}(\text{CH}_3)\text{--O--CF}_2\text{--CFH--CF}_3$ . This HFE was provided by Sumitomo-3M Limited (Osaka, Japan) and used as received. Powdery  $\beta$ -CD purchased from Wako Pure Chemical Industries., LTD (Osaka, Japan) was recrystallized from distilled water. An inclusion compound (IC) of HFE/ $\beta$ -CD was prepared as follows. HFE was mixed with a saturated aqueous solution of  $\beta$ -CD and stirred vigorously for 48 h at room temperature. The white powder thus precipitated was filtered, washed with distilled water, and dried in vacuo at 40 °C for 6 h. A portion of the sample was annealed by heating in air at 150 °C for 1 h and then cooled to room temperature.

### Nuclear magnetic resonance

Solid-state  $^{13}\text{C}$  and  $^{19}\text{F}$  NMR experiments were carried out on a Chemagnetics CMX-300 spectrometer running at resonance frequencies of 298.2, 279.9 and 75.0 MHz for

protons, fluorines and carbons, respectively, with a T3  $^1\text{H}/^{19}\text{F}/^{13}\text{C}$  triple-tune probe and 5 mm zirconia pencil rotors. The spinning speed was regulated at 8,000 Hz. Hexamethylbenzene was used for the external reference of  $^{13}\text{C}$  chemical shifts and the peak of the methyl group was set at 16.76 ppm from tetramethylsilane (TMS, 0 ppm). For  $^1\text{H} \rightarrow ^{13}\text{C}$  CP MAS NMR experiments, the proton  $\pi/2$  pulse width was set at 6.5  $\mu\text{s}$  with 2 ms of contact time and 15 s of recycle time. For  $^{19}\text{F} \rightarrow ^{13}\text{C}$  CP/MAS experiments, the fluorine  $\pi/2$  pulse width was set at 3.5  $\mu\text{s}$  with 5 ms of contact time and 15 s of recycle time. Solid-state  $^1\text{H}$  and  $^{19}\text{F}$  NMR experiments were performed on a JEOL EX spectrometer operating at resonance frequencies of 286.7 and 300.4 MHz for fluorines and protons, respectively, with a Chemagnetics APEX  $^{19}\text{F}/^1\text{H}$  dual-tune probe and 4 mm zirconia pencil rotors. The spinning speed was controlled at 15.0 kHz, and the fluorine  $\pi/2$  pulse width was set at 2.9  $\mu\text{s}$ .  $^{19}\text{F}$  chemical shifts were referenced to the  $\text{CF}_2$  peak of fluorosilicone rubber assigned to  $-66.30$  ppm from  $\text{CFCl}_3$  (0 ppm). A liquid HFE, which was soaked in cotton batting, was packed in a zirconia rotor. The temperature was calibrated using ethylene glycol adsorbed on tetrakis(trimethylsilyl)silane.

### X-ray diffraction

The WAXD patterns of  $\beta$ -CD and annealed HFE/ $\beta$ -CD were collected by Rigaku ULTIMA IV, where Cu-K $\alpha$  sources ( $\lambda = 0.154$  nm) were employed with a scanning speed of 0.5° min $^{-1}$ , and the applied voltage and current were set at 40 kV and 40 mA, respectively. The transmission WAXD experiments of HFE/ $\beta$ -CD were carried out at the Japan Synchrotron Radiation Research Institute (SPring-8) with a BL40B2 beam line using an image plate as the detector. The wavelength of the X-ray was set at 0.8 Å.

### Thermal analysis

TGA of  $\beta$ -CD and HFE/ $\beta$ -CD were performed with a Shimadzu DTG-60 in a temperature range from 30 to 700 °C at a heating rate of 10 °C min $^{-1}$ . TG–MS analysis was also carried out with a Shimadzu GCMS-QP60 equipped with a Rigaku Thermo plus EVO in a temperature range of 30–500 °C at a heating rate of 3 °C min $^{-1}$ . Dried nitrogen was purged during the above analysis.

## Results and discussion

Figure 1 shows the WAXD patterns of (a)  $\beta$ -CD and (b) HFE/ $\beta$ -CD IC with assignments of Miller indices. It has been reported that crystalline  $\beta$ -CD has a cage-type

structure [13] in the cavity of which some water molecules are incorporated [2, 14, 15]. Moreover, various types of crystalline structures of ICs have been reported, and they are categorized into four classes based on their packing structures; (1) channel, (2) screwed channel, (3) chess board, and (4) intermediate types [16, 17]. The major diffraction peaks of HFE/ $\beta$ -CD in Fig. 1b were reasonably consistent with those of 2,2'-vinylenedipyridine/ $\beta$ -CD IC [18] crystallized as a screwed channel structure, in which the axis penetrating the  $\beta$ -CD torus is slightly tilted from the *b* axis. Thus, the crystalline structure of HFE/ $\beta$ -CD can be classified as a screwed channel-type, which is the typical form for CD ICs, including relatively large guest molecules [2, 18, 19]. As we will discuss later, the structural change from the cage-type ( $\beta$ -CD) to the screwed channel-type (HFE/ $\beta$ -CD) can be attributed to the fact that two  $\beta$ -CD molecules capture a single guest molecule into the cavity.

Figure 2 shows the  $^1\text{H} \rightarrow ^{13}\text{C}$  CP MAS NMR spectra of  $\beta$ -CD and HFE/ $\beta$ -CD with signal assignments. Schematic structures of  $\beta$ -CD and HFE are inserted in the figure with atom labels, and the three chiral carbons of HFE are marked with asterisks. The  $^{13}\text{C}$  signals of  $\beta$ -CD were assigned by Zejli [20] and Li et al. [21]. For detecting a well-resolved  $^{13}\text{C}$  spectrum of HFE/ $\beta$ -CD, dual-frequency high-power decoupling was applied to  $^1\text{H}$  and  $^{19}\text{F}$  nuclei during signal acquisition for reducing dipolar interactions among  $^1\text{H}$ ,  $^{19}\text{F}$ , and  $^{13}\text{C}$  spins. In Fig. 2b, two weak peaks were newly observed in the ranges of 10–20 and 110–125 ppm, which are assignable to C5' and Ca' (C1', C3', C6' and C8') carbons of the HFE guest included in  $\beta$ -CD. Note that these new signals were not observed

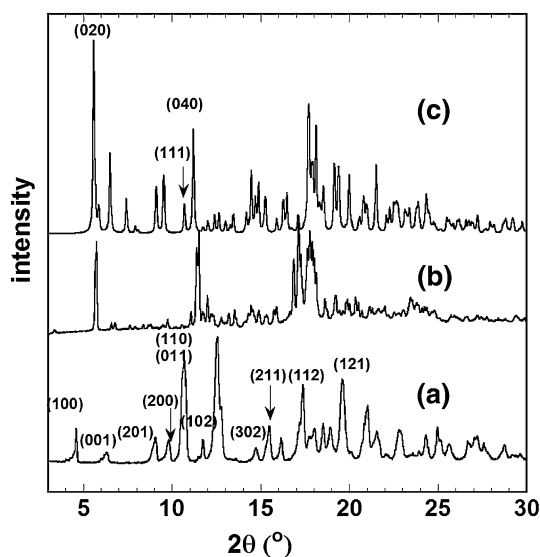


**Fig. 1** WAXD patterns of **a**  $\beta$ -CD, **b** HFE/ $\beta$ -CD and **c** 22VD/ $\beta$ -CD [18] with assignments of Miller indices

without  $^{19}\text{F}$  decoupling due to the strong  $^{19}\text{F}$ - $^{13}\text{C}$  interactions in the solid-state. Comparing the NMR spectra of both samples, the C1 signal of  $\beta$ -CD showed a broad shoulder at a lower frequency (ca. 95 ppm), whereas the C1 signal of HFE/ $\beta$ -CD showed a slightly smaller dispersion. This suggests that the structural distortion around the torus of crystalline  $\beta$ -CD was partially relaxed by the inclusion of the guest molecule, leading to a more ordered structure of  $\beta$ -CD IC [22]. It should be noted that the C1, C4 and C6 peaks (104.5, 82.4, 61.5 ppm, respectively) of HFE/ $\beta$ -CD IC resonate at higher frequencies than those of  $\beta$ -CD (103.6, 82.8, 62.3 ppm). In particular, it is noteworthy that the anomeric C1 carbon of IC was shifted by ca. 1.0 ppm. Horii and co-workers [23] demonstrated that the  $^{13}\text{C}$  chemical shifts of C1 and C4 in  $\beta$ -(1  $\rightarrow$  4)glucans are correlated with the torsion angles  $\Phi$  and  $\Psi$  (the definitions of  $\Phi$  and  $\Psi$  are shown in Scheme 1). Gidley et al. [24] also reported that the parameter can be used to evaluate the  $^{13}\text{C}$  chemical shifts of anomeric carbon (C1) [24–26]. Thereby, the high frequency shifts of C1 carbon observed for HFE/ $\beta$ -CD in this study suggest that the conformation of the  $\beta$ -CD ring was changed by inclusion of the HFE guest [24].

The magnetization dynamics of  $^{19}\text{F} \rightarrow ^{13}\text{C}$  CP is useful to investigate the structure and mobility of fluoropolymers [25], in particular to infer the apparent distances between the  $^{19}\text{F}$  and  $^{13}\text{C}$  nuclei. Figure 3 shows the  $^{19}\text{F} \rightarrow ^{13}\text{C}$  CP MAS spectra of HFE/ $\beta$ -CD observed with different contact

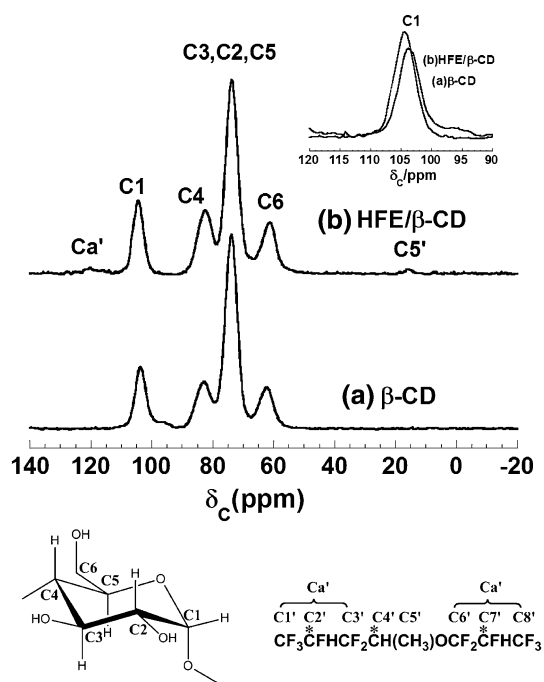
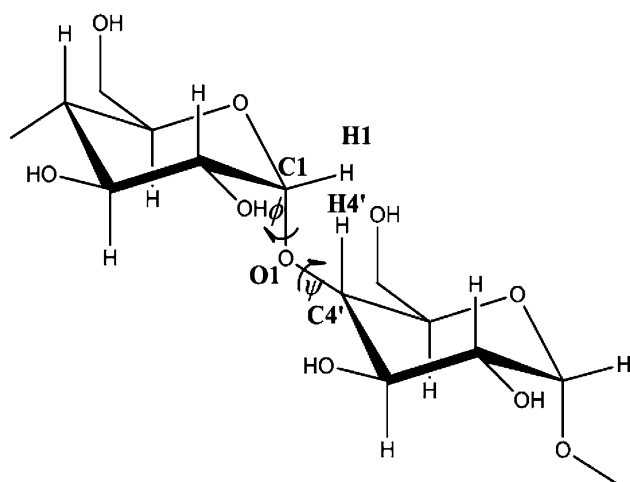


**Fig. 2**  $^1\text{H} \rightarrow ^{13}\text{C}$  CP/MAS NMR spectra of  $\beta$ -CD and HFE/ $\beta$ -CD.; Experimental: MAS rate, 8 kHz; data points, 1024; recycle delay, 15 s; 10,000 transients



**Scheme 1** Structural image of conformation associated with the glycosidic linkage in  $\alpha$ -(1  $\rightarrow$  4)-glucans. Torsion angle  $\phi$  is described by (H1)–(C1)–(O1)–(C4'), and angle  $\psi$  is described by (H4')–(C4')–(O1)–(C1)

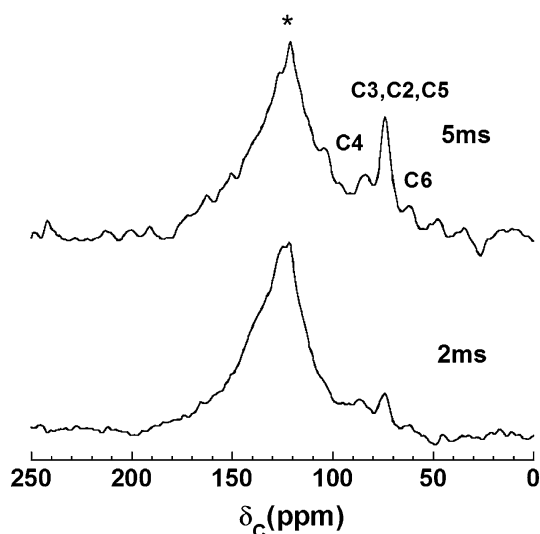


**Fig. 3**  $^{19}\text{F} \rightarrow ^{13}\text{C}$  CP/MAS NMR spectra of HFE/ $\beta$ -CD with various contact times: 2 and 5 ms.; Experimental: MAS rate, 8 kHz; data points, 1024; recycle delay, 15 s; 10,000 transients

times ( $t_{\text{cp}}$ ) for (a) 2 ms and (b) 5 ms. The broad signal at 125 ppm (marked by an asterisk) arises from a Teflon spacer of a MAS rotor. In both spectra, the C2, C3 and C5 peaks of  $\beta$ -CD are observed in the range of 70–80 ppm, though the signal intensities are much larger for  $t_{\text{cp}} = 5$  ms than  $t_{\text{cp}} = 2$  ms, and the C4 and C6 signals were clearly detected in the former. This indicates that effective heteronuclear polarization transfer occurred between the  $^{19}\text{F}$  nuclei in HFE and the  $^{13}\text{C}$  nuclei of  $\beta$ -CD, suggesting that HFE guest molecules are spatially located very close to  $\beta$ -CD hosts, which also strongly support the inclusion of HFE in the cavity of  $\beta$ -CD.

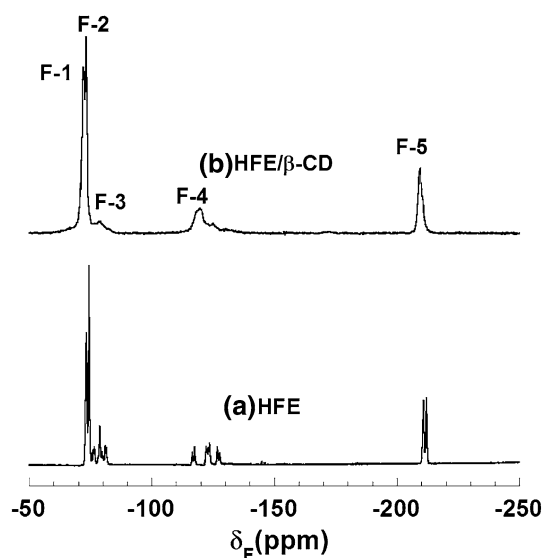


**Fig. 4** Liquid-state  $^{19}\text{F}$  NMR spectra and Solid-state  $^{19}\text{F}$  MAS NMR of HFE/ $\beta$ -CD; Experimental: data points, 2048; recycle delay, 5 s

Figure 4 shows the solid-state direct polarization (DP)  $^{19}\text{F}$  MAS NMR spectrum of HFE/ $\beta$ -CD and the liquid-state  $^{19}\text{F}$  NMR spectrum of neat HFE at 40  $^{\circ}\text{C}$ . Although continuous wave (CW)  $^1\text{H}$  decoupling was applied to the liquid  $^{19}\text{F}$  spectrum, multi-splitting of signals was not eliminated. This indicates that the splitting was caused by the existence of plural stereo-isomers of HFE. HFE could be a mixture of eight kinds of isomers generated by three chiral centers. Thereby, all peaks were assigned on the basis of quantum chemical density functional theory (DFT) calculations [26]. In the  $^{19}\text{F}$  MAS spectrum of HFE/ $\beta$ -CD, such multi-splitting peaks from HFE turn into broad signals, reflecting the restricted mobility of HFE in the ICs. Note that all the  $^{19}\text{F}$  signals of HFE/ $\beta$ -CD resonate at higher frequencies than those of neat HFE liquid by 1.1, 1.2, and 2.6 ppm for F1, F2 and F5 signals, respectively. This agrees with the fact that all the  $^{19}\text{F}$  signals for  $\text{C}_9\text{F}_{20}/\beta$ -CD resonate at higher frequencies than those for neat  $\text{C}_9\text{F}_{20}$ , as we previously reported [12]. A presumable factor that causes the chemical shift change is the ‘dielectric media effect’ which is similar to the ‘solvent effect’ frequently observed in solution NMR. Since the inside environment of a CD cavity is less polar and more hydrophobic than the outside, the fluorine nuclei of HFE in the IC host were significantly deshielded. As stated below, this is supported by the DFT calculation of  $^{19}\text{F}$  nuclear shieldings of the HFE molecule entering into a cavity of  $\beta$ -CD.

Elemental analysis was carried out to determine the precise atomic ratio of fluorine to carbon of HFE/ $\beta$ -CD IC, which was estimated to be 4.91. This value confirms that the ratio of the HFE guest to the  $\beta$ -CD host is almost equal to 1: 2 because the F/C ratio of the ideal 1:2 complex is 4.84. Based on these results, we can conclude that one HFE

molecule is included in two  $\beta$ -CD rings, which forms a channel-type IC in the solid-state.

As stated in the Introduction, the thermal stability of HFE/ $\beta$ -CD IC is an important property for practical applications. The TGA curves for  $\beta$ -CD and HFE/ $\beta$ -CD IC are shown in Fig. 5a. A weight loss of 9.0 % was observed up to 120 °C for  $\beta$ -CD, followed by a plateau ranging from 120 to 280 °C, and significant thermal degradation occurred above 280 °C. This behavior is consistent with that reported in the previous works [27, 28]. In the case of HFE/ $\beta$ -CD IC, the sample weight was gradually decreased from room temperature to 280 °C, and the weight losses at 100 and 280 °C were only 5.5 and 10.8 %, respectively. At almost the same temperature range as  $\beta$ -CD, significant thermal degradation occurred above 300 °C [29]. Furthermore, TG-MS was performed to identify decomposed species or fragments of the IC at elevated temperatures. Figure 5b indicates the multiple ion detection (MID) curves of five representative fragments for HFE/ $\beta$ -CD IC. For reference, several fragment ions related to HFE and  $\beta$ -CD are summarized in Table 1. The fragments of  $m/e = 18$  and 44 correspond to water and a glucopyranose unit of  $\beta$ -

**Table 1** Fragments related the decomposition of HFE/ $\beta$ -CD

Fragments	$m/e$ unit
$\text{OH}_2^+$	18
$\text{HOCH}_2\text{CH}^+$	44
$\text{CF}_3^+$	69
$\text{CF}_3\text{CFHCF}_2^+$	151
$\text{CF}_3\text{CFHCF}_2\text{CH}(\text{CH}_3)\text{O}^+$	195

CD, respectively [30]. The fragments of  $m/e = 69$ , 151 and 195, which are attributable to HFE molecules, were not detected until HFE/ $\beta$ -CD IC was thermally degraded at around 300 °C. This clearly indicates that the weight loss of HFE/ $\beta$ -CD IC below 300 °C is mainly caused by desorption of water molecules captured inside the  $\beta$ -CD rings or the crystalline water of ordered  $\beta$ -CD structures. These results clearly demonstrate that HFE/ $\beta$ -CD IC has high thermal stability, and HFE molecules included inside the cavity of  $\beta$ -CD are preserved even at higher temperatures than the boiling point of HFE (131 °C).

Figure 6 shows the  $^{19}\text{F}$  DP MAS NMR spectra of HFE/ $\beta$ -CD, as prepared (a) and annealed at 150 °C (b). After annealing, the signals of F1, F2 and F5 were shifted to higher frequencies by 0.9, 1.1, and 1.5 ppm, respectively (see Fig. 6b). In addition, the spectral widths of these signals became slightly broader than those in the initial state, suggesting that annealing caused slight disordering in the conformation of HFE in the IC. To infer the reasons for the  $^{19}\text{F}$  signal displacements, calculation of nuclear shieldings based on DFT may give useful information. In a

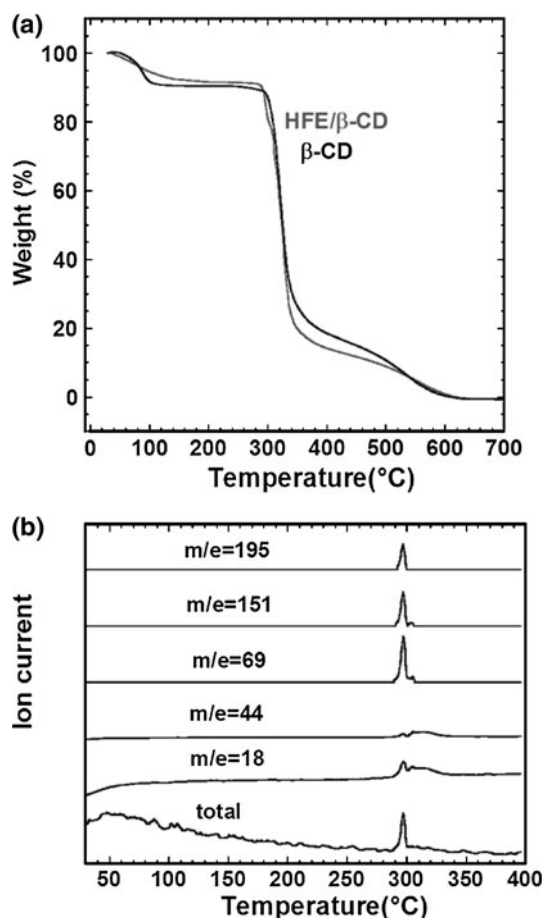


**Fig. 5** a TGA curves for  $\beta$ -CD and HFE/ $\beta$ -CD and b MID curves of HFE/ $\beta$ -CD

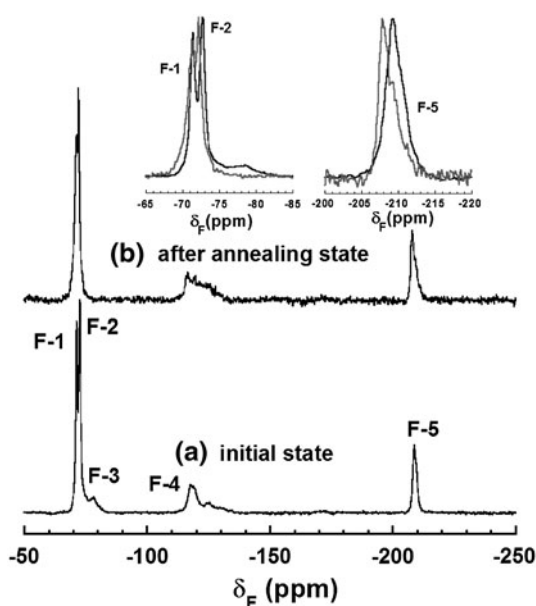


**Fig. 6**  $^{19}\text{F}$  NMR spectra of HFE/ $\beta$ -CD at initial and post annealing state.; Experimental: MAS rate, 15 kHz; data points, 1024; recycle delay 5 s

model system, one HFE molecule was initially placed in the cavity of one  $\beta$ -CD, and it was linearly moved and inserted into the cavity, as shown in Fig. 7a. The stick spectra of the calculated  $^{19}\text{F}$  nuclear shielding of the HFE molecule are displayed in Fig. 7b. As the HFE molecule

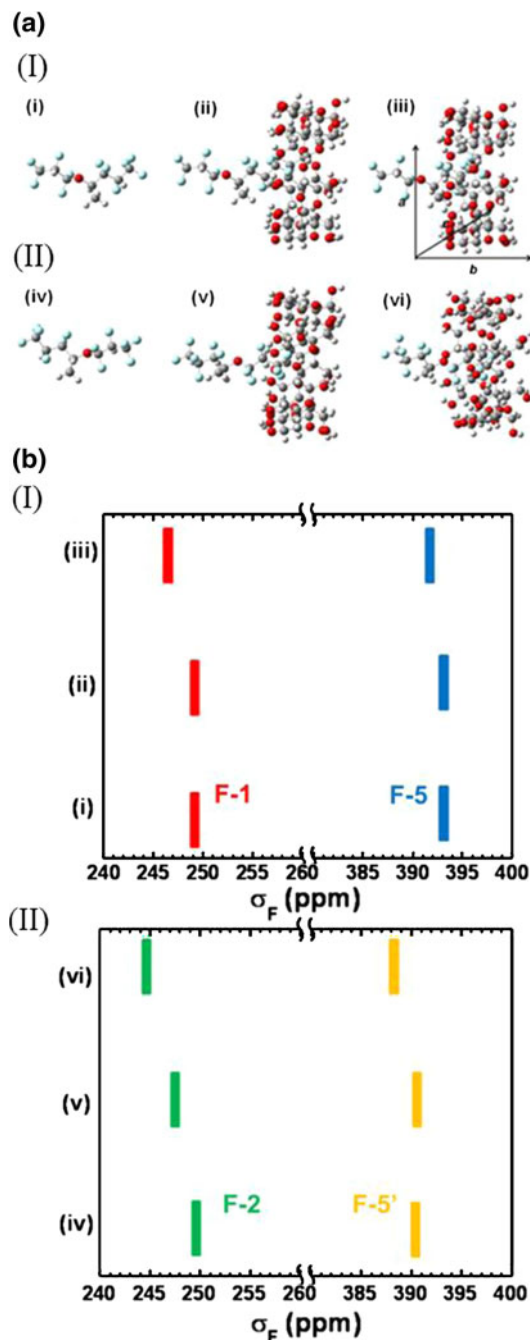


**Fig. 7** **a** Structural image of HFE/ $\beta$ -CD IC with different included state between HFE and  $\beta$ -CD molecules. Models included from the side of  $\text{CF}_3$ (F-1) (I): (i), (ii), (iii) and from the side of  $\text{CF}_3$ (F-2) (II): (iv), (v), (vi) and **b** Stick spectra for each model demonstrating the calculated  $^{19}\text{F}$  magnetic shielding of (I) F-1, F-5 and (II) F-2, F-5' corresponding to (a)

enters deeper into the cavity of  $\beta$ -CD, all the  $^{19}\text{F}$  positions are shifted to lower shielding, which corresponds to higher frequency shifts. Thereby, the higher frequency shifts observed in Fig. 6 indicate that the distance between the guest (HFE) and host ( $\beta$ -CD) molecules was further reduced by annealing.

Figure 8 shows the WAXD patterns of HFE/ $\beta$ -CD (a) and annealed HFE/ $\beta$ -CD (b). After annealing at 150 °C, broadening of each peak was observed, which could be caused by disordering of the crystal structure of HFE/ $\beta$ -CD. It was also observed that the diffraction peaks indexed as (020) and (040), which reflect ordering along the  $b$  axis, were shifted to higher angles after annealing. According to the crystal structure simulation using Mercury 2.4 software [31] based on the crystalline parameters estimated from HFE/ $\beta$ -CD (Fig. 1b) and 22VD/ $\beta$ -CD [18], the periodic structure along the direction penetrating the  $\beta$ -CD torus ( $b$  axis) was shortened, and the (020) peak was shifted from 5.75° to 6.08° after annealing. In other words, the  $d$ -spacing of (020) ( $d_{020}$ ) was changed from 15.36 to 14.32 Å. The crystalline model structure based on the WAXD pattern agrees well with the shortening of the crystal packing of HFE/ $\beta$ -CD ICs only along the  $b$  axis, not the  $a$ - or  $c$ -axes. These findings from solid-state  $^{19}\text{F}$  MAS NMR and X-ray diffraction clearly demonstrate that the packing structure of the crystalline HFE/ $\beta$ -CD IC was tighter along the  $b$  axis around 150 °C, and the HFE molecules included in the ICs were kept within the ICs up to 280 °C without molecular degradation. As a consequence, the structural changes occurring at relatively lower temperatures (<150 °C) generated tightly packed and energetically stable structures of HFE/ $\beta$ -CD IC, which were endowed with high thermal stability.

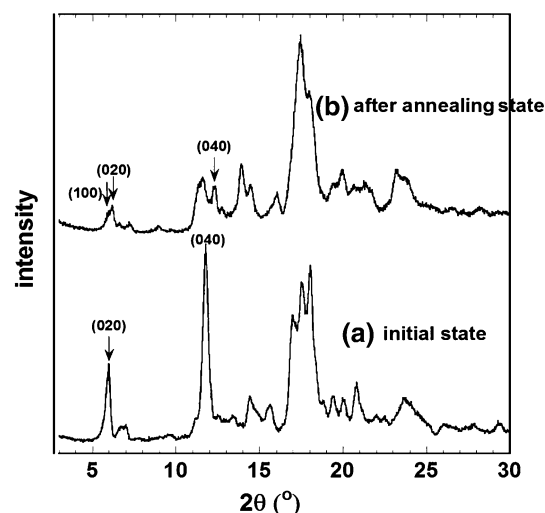


**Fig. 8** WAXD patterns of HFE/ $\beta$ -CD at initial and post annealing state

## Conclusions

An IC composed of one HFE guest molecule included in two  $\beta$ -CD host molecules was prepared, and the structure at room temperature and the structural changes generated at elevated temperatures were characterized by WAXD, solid-state  $^{13}\text{C}$  and  $^{19}\text{F}$  MAS NMR, TGA, TG–MS, and elemental analysis. The formation of HFE/ $\beta$ -CD IC was confirmed by a WAXD pattern indicating a channel-type structure, appearance of HFE signals in the  $^{19}\text{F} \rightarrow ^{13}\text{C}$  CP MAS NMR spectrum, and a high frequency shift of HFE signals in the  $^{19}\text{F}$  MAS NMR caused by formation of IC. According to TG analysis, HFE molecules included in  $\beta$ -CD were hardly evaporated or degraded below the decomposition temperature of the host at around 300 °C. In contrast, the  $^{19}\text{F}$  NMR signals of HFE included IC were resonated at higher frequencies after annealing at 150 °C. With the aid of DFT calculations, these results evidenced that HFE molecules were more deeply included into a  $\beta$ -CD cavity by annealing. WAXD pattern also showed that diffraction peaks along  $b$  axis, such as (020) and (040), were shifted to higher angles after annealing, indicating that the crystal packing of ICs became tighter along the direction penetrating the torus of  $\beta$ -CD, which agrees with the result of  $^{19}\text{F}$  MAS NMR analysis. Accordingly, HFE molecules are more likely to remain in ICs with tight packing after annealing without removing from the ICs. This knowledge is valuable for application of  $\beta$ -CD IC as a removal agent of fluorine-containing compounds based on its capacity of trapping molecules up to high temperatures.

**Acknowledgments** The synchrotron radiation experiments were performed with a BL40B2 beam line with the approval of the Japan Synchrotron Radiation Research Institute (JASRI) (Proposal 2009A-1348, 2009B-1306). The authors thank Noboru Ohta at the Japan Synchrotron Radiation Research Institute (JASRI)/SPring-8 for support and advice on the synchrotron WAXD measurements. The authors also thank Kenzo Deguchi at the National Institute for Materials Science and Shigeki Kuroki at the Tokyo Institute of Technology for technical assistance on solid-state NMR and TG–MS measurements.

## References

- Danielsson, J., Javet, J., Damberg, P., Gräslund, A.: Two-site binding of  $\beta$ -cyclodextrin to the Alzheimer A $\beta$ (1–40) peptide measured with combined PFG-NMR diffusion and induced chemical shifts. *Biochemistry* **43**, 6261–6269 (2004)
- Harata, K.: Structural aspects of stereodifferentiation in the solid state. *Chem. Rev.* **98**, 1803–1828 (1998)
- Hollowell, J.G., Staehling, N.W., Flanders, W.D., Gunter, E.W., Spencer, C.A., Braverman, L.E.: Serum TSH, T4, and thyroid antibodies in the United States population (1988 to 1994): national health and nutrition examination survey (NHANES III). *J. Clin. Endocrinol. Metab.* **87**, 489–499 (2002)
- Misale, M., Guglielmini, G., Priarone, A.: HFE-7100 pool boiling heat transfer and critical heat flux in inclined narrow spaces HFE-7100. *Int. J. Refrig.* **32**, 235–245 (2009)
- Christensen, L.K., Sehested, J., Nielsen, O.J., Bilde, M., Wallington, T.J., Guschin, A., Molina, L.T., Molina, M.J.: Atmospheric chemistry of HFE-7200 ( $\text{C}_4\text{F}_9\text{OC}_2\text{H}_5$ ): reaction with OH radicals and fate of  $\text{C}_4\text{F}_9\text{OCH}_2\text{CH}_2\text{O}(\cdot)$  and  $\text{C}_4\text{F}_9\text{OCHO}(\cdot)\text{CH}_3$  radicals. *J. Phys. Chem. A* **102**, 4839–4845 (1998)
- Martinez-Haya, B., Hurtado, P., Hortal, A.R., Hamad, S., Steill, J.D., Oomens, J.: Emergence of symmetry and chirality in crown ether complexes with alkali metal cations. **114**, 7048–7054 (2010)
- Shinkai, S., Araki, K., Manabe, O.: Does the calixarene cavity recognise the size of guest molecules? On the ‘hole-size selectivity’ in water-soluble calixarenes. *J. Chem. Soc. Chem. Commun.* **3**, 156–158 (1988)
- Silva, D.L., Tavares, E.C., Conegero, L.S., Fatima, A., Pilli, R.A., Fernandes, S.A.: NMR studies of inclusion complexation of pyrrolizidine alkaloid retronecine and  $p$ -sulfonic acid calix[6] arene. *J. Incl. Phenom. Macrocycl. Chem.* **69**, 149–155 (2011)
- Lu, J., Shin, I.D., Nojima, S., Tonelli, A.E.: Formation and characterization of the inclusion compounds between poly( $\epsilon$ -caprolactone)-poly(ethylene oxide)-poly( $\epsilon$ -caprolactone) triblock copolymer and  $\alpha$ - and  $\gamma$ -cyclodextrin. *Polymer* **41**, 5871–5883 (2000)
- Lu, J., Mirau, P.S., Shin, I.D., Nojima, S., Tonelli, A.E.: Molecular motions in the supramolecular complexes between poly( $\epsilon$ -caprolactone)-poly(ethylene oxide)-poly( $\epsilon$ -caprolactone) and  $\alpha$ - and  $\gamma$ -cyclodextrins. *Macromol. Chem. Phys.* **203**, 71–79 (2002)
- Saalwächter, K.: An investigation of poly(dimethylsiloxane) chain dynamics and orders in its inclusion compound with  $\gamma$ -cyclodextrin by fast-MAS solid-state NMR spectroscopy. *Macromol. Rapid Commun.* **23**, 286–291 (2002)
- Tatsuno, H., Ando, S.: Structure and dynamics of perfluoroalkane/ $\beta$ -cyclodextrin inclusion compounds as studied by solid-state  $^{19}\text{F}$  MAS and  $^1\text{H} \rightarrow ^{19}\text{F}$  CP/MAS NMR spectroscopy. *J. Phys. Chem. B.* **110**, 25751–25760 (2006)
- Lindner, K., Saenger, W.:  $\beta$ -Cyclodextrin dodecahydrate: crowding of water molecules within a hydrophobic cavity. *Angew. Chem. Int. Ed.* **17**, 694–695 (1978)
- Steiner, T., Koellner, G.: Crystalline beta-cyclodextrin hydrate various humidities: fast continuous, and reversible dehydration studied by X-ray diffraction. *J. Am. Chem. Soc.* **116**, 5122–5128 (1994)
- Lindner, K., Saenger, W.: Crystal and molecular structure of cyclohepta-amylose dodecahydrate. *Carbohydr. Res.* **99**, 103–105 (1982)
- Bojinova, T., Gornitzka, H., Viguerie, N.L., Rico-Lattes, I.: Crystal structure of the dimeric  $\beta$ -cyclodextrin complex with 1,12-dodecanediol. *Carbohydr. Res.* **338**, 781–785 (2003)
- Mentzafos, D., Mavridis, I.M., Le Bas, I.G., Tsoucaris, G.: Structure of the 4-*tert*-butylbenzyl alcohol- $\beta$ -cyclodextrin dimeric complexes. *Acta Crystallogr. Sect. B* **47**, 746–757 (1991)
- Zhao, Y.L., Benitez, D., Yoon, I., Stoddart, J.F.: Inclusion behavior of  $\beta$ -cyclodextrin with bipyridine molecules: factors governing host-guest inclusion geometries. *Chem. Asian J.* **4**, 446–456 (2009)
- Giastar, P., Yannakopoulou, K., Mavridis, I.M.: Molecular structures of the inclusion complexes  $\beta$ -cyclodextrin-1,2-bis(4-aminophenyl)ethane and  $\beta$ -cyclodextrin-4,4'-diaminobiphenyl; packing of dimeric  $\beta$ -cyclodextrin inclusion complexes. *Acta Crystallogr. Sect. B* **59**, 287–299 (2003)
- Zejli, S.: Introduction and general overview of cyclodextrin chemistry. *Chem. Rev.* **98**, 1743–1754 (1998)
- Li, N., Liu, J., Zhao, X., Gao, Y., Zheng, L., Zheng, J., Yu, L.: Complex formation of ionic liquid surfactant and  $\beta$ -cyclodextrin. *Colloids Surf. A* **292**, 196–201 (2007)

22. Sfihi, H., Legrand, A.P., Doussot, J., Guy, A.: Solid-state  $^{13}\text{C}$  NMR study of  $\beta$ -cyclodextrin/substituted aromatic ketone complexes: evidence for two kinds of complexation of the guest molecules. *Colloids Surf. A* **115**, 115–126 (1996)
23. Horii, F., Hirai, A., Kitamaru, R.: Relationships between carbon-13 chemical shifts and conformations of oligosaccharides and cellulose in the solid state. *Bull. Magn. Reson.* **5**, 190 (1983)
24. Gidly, M.J., Bociek, S.M.: Carbon-13 CP/MAS NMR studies of amylose inclusion complexes, cyclodextrins, and the amorphous phase of starch granules: relationships between glycosidic linkage conformation and solid-state carbon-13 chemical shifts. *J. Am. Chem. Soc.* **110**, 3820–3829 (1988)
25. Jarvis, M.C.: Relationship of chemical shift to glycosidic conformation in the solid-state  $^{13}\text{C}$  NMR spectra of (1  $\rightarrow$  4)-linked glucose polymers and oligomers: anomeric and related effects. *Carbohydr. Res.* **259**, 311–318 (1994)
26. Zhang, P., Klymachyov, A.N., Brown, S., Ellington, J.G., Grandinetti, P.J.: Solid-state  $^{13}\text{C}$  NMR investigations of the glycosidic linkage in  $\alpha$ - $\alpha'$  trehalose. *Solid State Nucl. Magn. Reson.* **12**, 221–225 (1998)
27. Szafranex, A., Szafranex, J.: Thermogravimetric properties of inclusion complexes of  $\beta$ -cyclodextrin with benzene, acetylsalicylic acid and methyl salicylate. *J. Incl. Phenom. Mol.* **15**, 351–358 (1993)
28. Giordano, F., Mnpvac, C., Moyano, J.R.: Thermal analysis of cyclodextrins and their inclusion compounds. *Thermochim. Acta.* **123**, 123–151 (2001)
29. Trotta, F., Zanetti, M., Camino, G.: Thermal degradation of cyclodextrins. *Polym. Degrad. Stab.* **69**, 373–379 (2000)
30. Éhen, Z., Giordano, F., Sztatisz, J., Jinsinszky, L., Novák, C.: Thermal characterization of natural and modified cyclodextrins using TG–MS combined technique. *J. Therm. Anal. Cal.* **80**, 419–424 (2005)
31. Macrae, C.F., Bruno, I.J., Chisholm, J.A., Edgington, P.R., McCabe, P., Pidcock, E., Rodriques Monge, L., Taylor, R., van de Streek, J., Wood, P.A.: Mercury CSD 2.0—new features for the visualization and investigation of crystal structures. *J. Appl. Cryst.* **41**, 466–470 (2008)